ISTITUTO NAZIONALE DI FISICA NUCLEARE - ISTITUTO NAZIONALE DI FISICA NUCLEARE - ISTITUTO NAZIONALE DI FISICA NUCLEARE - ISTITUTO NAZIONALE DI FISICA NUCLEARE - ISTITUTO NAZIONALE DI FISICA NUCLEARE - ISTITUTO NAZIONALE DI FISICA NUCLEARE - ISTITUTO NAZIONALE DI

Laboratori Nazionali di Frascati

Submitted to Particle Accelerator

LNF-93/067 (P)
15 Ottobre 1993

S. Bartalucci, M. Bassetti, R. Boni, S. De Santis, A. Drago, A. Gallo,
A. Ghigo, M.Migliorati, L. Palumbo , R. Parodi, M. Serio, B. Spataro,
G. Vignola, M. Zobov:

ANALYSIS OF METHODS FOR CONTROLLING MULTIBUNCH INSTABILITIES IN DAΦNE

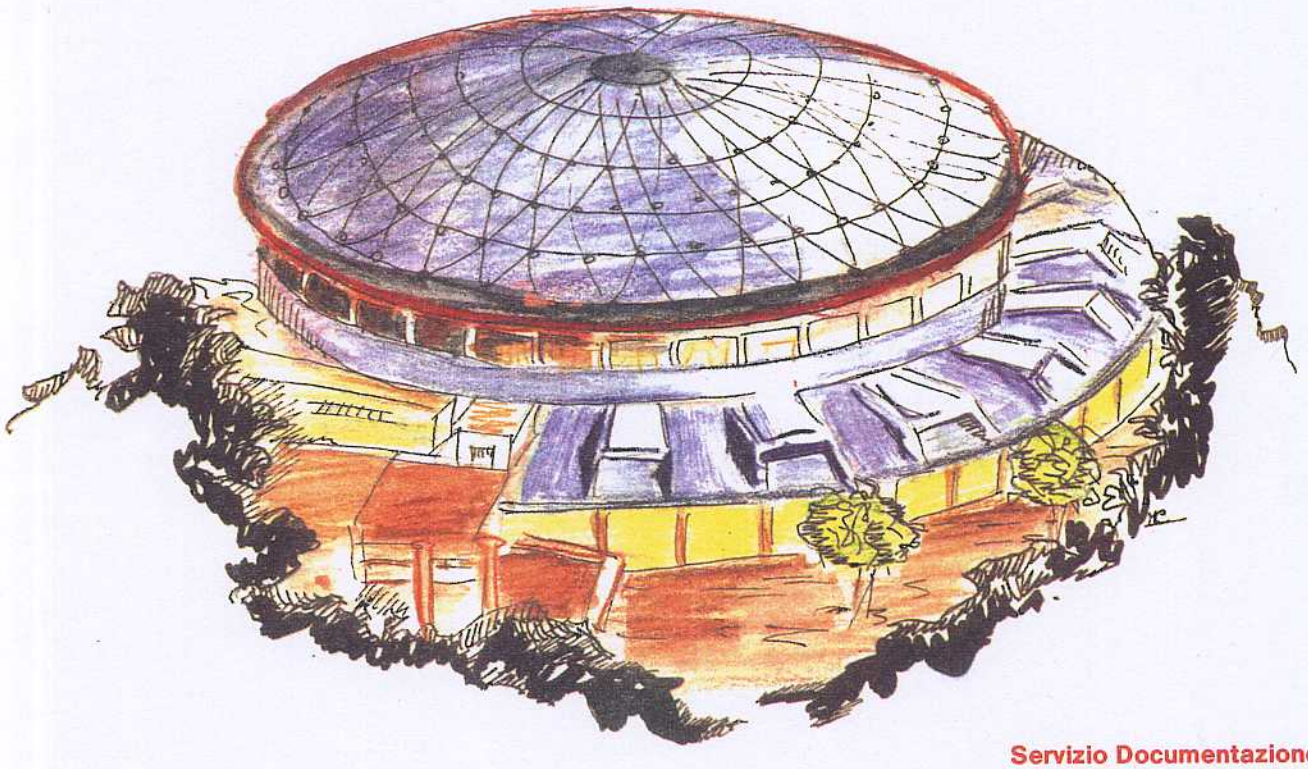

Servizio Documentazione
dei Laboratori Nazionali di Frascati
P.O. Box, 13 - 00044 Frascati (Italy)

INFN - Laboratori Nazionali di Frascati
Servizio Documentazione

LNF-93/067 (P)
15 Ottobre 1993

ANALYSIS OF METHODS FOR CONTROLLING MULTIBUNCH INSTABILITIES IN DAΦNE

S. Bartalucci*, M. Bassetti*, R. Boni*, S. De Santis°, A. Drago*, A. Gallo*, A. Ghigo*, M.Migliorati*, L. Palumbo*° , R. Parodi #, M. Serio*, B. Spataro*, G. Vignola*, M. Zobov*

(*) INFN-Laboratori Nazionali di Frascati, C.P. 13, 00044 Frascati, Italy
(°) Dip. di Energetica, Universita' La Sapienza, Roma, Italy
(#) INFN - Sezione di Genova, Via Dodecaneso 33, 16146 Genova, Italy

Abstract

The e^-e^+ DAΦNE collider is designed to reach a luminosity of the order of 10^{32}-10^{33} [sec^{-1} cm^{-2}] at 510MeV, by storing high current. Such a current, of the order of few amperes for beam, can in principle be achieved by filling many RF buckets in the machine. One of the main problems arising in the beam dynamics concerns the Multibunch Instabilities caused by the strong coupling between the beam and the parasitic HOM resonances of the RF cavity. Due to the high current, the instability is very fast, so that it is impossible to stabilize the beam with a feedback system alone. An effort has to be made to reduce the shunt impedance of the cavity HOMs, so that a feedback system can be effective. This task is accomplished by properly designing the RF cavity and by coupling off the HOMs through loops or waveguides in order to extract energy from the resonant fields, thus reducing at the same time the quality factor Q and the shunt impedance R. The residual excitation of beam oscillations is damped by means of a bunch-by-bunch digital feedback system.

Used symbols

α_c	Momentum compaction.
α_1	Dipole oscillations growth rate ($1/\tau_1$).
α_{eff}	Effective dipole oscillations growth rate ($1/\tau_{eff}$).
α_f	HOM filling rate.
α_{fb}	Feedback damping rate.
β	Natural angular frequency for a single HOM.
ΔE	Energy deviation.
ΔU_{fb}	Feedback energy correction.
$\Delta\varphi$	Phase angle of synchrotron oscillations.
$\Delta\Psi_m$	Coherent mode of oscillation m^{th}.
e	Electron charge.
E	Nominal electron energy.
$\mathbf{E}_w(\mathbf{r})$	Waveguide electric field.
$\mathbf{G}_m(\mathbf{r},\mathbf{r}')$	Magnetic Green function for a rectangular waveguide (3 X 3 matrix).
$g_o(\tau)$	Stationary longitudinal phase space distribution.
h	Harmonic number.
$\mathbf{H}_o(\mathbf{r})$	Cavity unperturbed magnetic field.
$\mathbf{H}_w(\mathbf{r})$	Waveguide magnetic field.
i(t)	Induced wake current in the inductance of a single HOM.
$i_o(t)$	Beam current.
I_o	Beam average current.
I_m	Amplitude of "m" armonics.
$\mathbf{J}_s(\mathbf{r})$	Current density.
$J_m(x)$	Bessel function of the first kind of m^{th} order.
k_{pm}	HOM loss factor.
k_b	Number of bunches.
n	relative mode number.
P_T	Total dissipated HOM power.
P_w	Total power dissipated in the waveguide loads.
Q	Cavity quality factor.
q_b	Bunch charge.
R	Cavity shunt resistance.
σ_t	RMS bunch duration.
τ	Longitudinal phase space amplitude.
τ_f	HOM Filling time.
τ_1	Dipole rise time.
τ_d	Longitudinal radiation damping time.
τ_{eff}	Effective dipole rise time.
$\bar{\tau}_{eff}$	Asymptotic effective rise time (for high Q).
U	Total energy of a single HOM.
U_{bb}	Energy loss for the broad band impedance.
U_o	Energy loss by radiation for the synchronous particle.
U_r	Energy loss by radiation.
v(t)	Induced wake voltage for a single HOM.
V_g	Generator voltage.
$Z(\omega)$	HOM impedance.
ω_o	Revolution angular frequency.
ω_c	Coherent synchrotron angular frequency.
ω_r	Resonance angular frequency for a single HOM.
ω_s	Incoherent synchrotron angular frequency.

1. - INTRODUCTION

In the Φ-Factory DAΦNE, a 510 MeV e^+e^- twin ring collider under construction at Frascati Laboratories (see Table I), the luminosity goal is achievable by storing a high current in many bunches. This has required a strong effort on the study of the control of multibunch instabilities. The problem can be afforded both from the side of the reduction of the causes and from the side of the cures of the instability.

Table I – DAΦNE single ring parameter list.

Machine length	97.69	(m)
Revolution freq.	3.069	(MHz)
RF frequency	368.26	(MHz)
Harmonic number	120	
Number of Bunches	30 ÷ 120	
V_{RF}	254	(KV)
Energy	510	(MeV)
Radiation loss/turn	9.32	(KeV)
Momentum compaction	$5.8*10^{-3}$	
Synchrotron frequency	22.88	(KHz)
RMS bunch duration	100	(psec)
Longitudinal damping time	17.8	(msec)

An analysis of the interaction of the beam spectrum with the parasitic modes of the RF cavity shows that the instability growth rates depend on the strength of the "stable" and "unstable" sidebands and their position with respect to the HOMs.

For HOMs with very high Qs, it is really unlikely that a sideband couples to an HOM. The shunt impedance of these HOMs also is very high, however harmless as long as the HOM is not excited by a sideband. Unfortunately during machine operation the HOM frequency can drift, because of thermal excursions or as a side effect of tuning the fundamental mode, leading to a strong coupling and very fast instability.

A careful design of the cavity shape can lead to HOMs with rather low shunt impedances $R/Q<1\Omega$, however not low enough to maintain the stability in case of full coupling.

Recent development of HOM damping techniques have shown that, for normal conducting cavities, it is possible to achieve Qs less than 100, thereby obtaining a strong reduction of the beam-HOM coupling. This would make it possible to damp the residual multibunch instabilities by means of a feedback system.

In this paper we describe the results obtained at the design stage for DAΦNE[1]. The work is organized as follows: in section 2 the theoretical estimates of the growth rates are presented; the optimum design of an RF cavity with low HOM contents is briefly described in section 3; the HOM damping techniques, which have been investigated, are treated in section 4; section 5 illustrates the bunch-by-bunch feedback system, while the time domain simulation code able to show the beam dynamics behavior and the effectiveness of the feedback system is described in section 6.

2. – THEORETICAL GROWTH RATES

2.1 – Coherent frequency shift

The analysis of the dynamics of k_b equispaced bunches interacting with the long range wake fields is performed by computing the coherent frequency shift predicted by Sacherer's theory[2].

Any perturbation of a bunch with a stationary phase space distribution $g_o(\tau)$ is developed as sum of multipole coherent modes $\Delta\Psi_m$. Under the effect of long range wakefields the coherent mode of oscillation "m" (m=1 dipole, m=2 quadrupole, etc.) can grow or decay in amplitude. Limiting our analysis to the dipole mode, we have

$$\Delta\Psi_1 = g_1(\tau)\exp[j(\omega_c - \omega_s)] \tag{1}$$

where $g_1(\tau)$ is the perturbation amplitude, and $(\omega_c - \omega_s)$ is the complex coherent angular frequency shift with respect to the synchrotron one ω_s.

The spectrum of the bunches executing free dipole oscillations exhibits lines at angular frequencies

$$\omega_p = (pk_b + n)\,\omega_o + \omega_s \tag{2}$$

$$-\infty < p < +\infty\,,\ 0 \le n \le k_b\text{-}1,\ p,n \text{ integers}$$

where n is the number of the relative mode of oscillation.

In DAΦNE, due to high revolution frequency, the unstable sidebands corresponding to a given "n", are quite apart. A single HOM with high Q can at most excite a single sideband. For a damped HOM, with Q≈100, the resonator can significantly couple to a few unstable sidebands. However, the bandwidth is such that, apart of $n \approx k_b/2$, there will not be compensation of stable and unstable sidebands.

In the following analysis we shall consider the effect of a single HOM coupling to the relative bunch motion "n". Let ω_r, R, Q be the resonator parameters. In this simple case the coherent frequency shift is[3]:

$$j(\omega_c - \omega_s) = -\frac{\alpha_c I_o}{\omega_s (E/e)} \frac{Z(q\,\omega_o + \omega_c)}{q} \int_o^\infty \frac{\partial g_o}{\partial \tau} J_1^2(q\,\omega_o \tau)\, d\tau \tag{3}$$

where I_o is the beam current, α_c the momentum compaction, $q = pk_b + n$, and

$$Z(q\,\omega_o + \omega_c) = \frac{R}{1 + jQ\left(\dfrac{q\omega_o + \omega_c}{\omega_r} - \dfrac{\omega_r}{q\omega_o + \omega_c}\right)} \tag{4}$$

the resonator impedance.

The customary way of computing the coherent frequency shift[4,5] considers the bunch spectrum at angular frequencies ω_p, i.e. the spectrum of a bunch with dipole perturbation executing free oscillations in the absence of growth or damping. Once the impedance spectrum is known, this procedure leads to the solution for the unknown ω_c. This is not exactly what is prescribed in eq.(3) where the impedance has to be computed at the shifted

frequencies. As a matter of fact, eq.(3) is an eigenvalue problem for ω_c. Computing the impedance at the bunch spectrum sidebands (2) leads to an estimate of the growth rates that is not exact, especially in the case of high Q resonances[6,7].

Let us write, for simplicity, eq.(3) in a more compact form

$$j(\omega_c - \omega_s) = \frac{\theta_1(q)}{q} Z(q\omega_o + \omega_c) I_o \tag{5}$$

with

$$\theta_1(q) = -\frac{\alpha_c}{\omega_s (E/e)} \int_o^\infty \frac{\partial g_o}{\partial \tau} J_1^2(q\omega_o \tau) d\tau \tag{6}$$

In the realistic case that $\omega_c << \omega_r$ the impedance can be approximated by:

$$Z(q\omega_o + \omega_c) \approx \frac{R}{1 + \frac{j\omega_c}{\alpha_f} + jtg(\Phi_r)} \tag{7}$$

where

$$\alpha_f = \frac{\omega_r}{2Q} \text{ and } tg(\Phi_r) = Q\left(\frac{q\omega_o}{\omega_r} - \frac{\omega_r}{q\omega_o}\right) \tag{8}$$

are the filling rate of the resonant mode ($\tau_f = 1/\alpha_f$ = filling time) and the detuning of the resonant mode with respect to the line "q" of the bunch spectrum, respectively.

With these definitions and approximations, the coherent tune shift is obtained by solving the following equation:

$$\omega_c^2 + \left[\alpha_f tg(\Phi_r) - \omega_s - j\alpha_f\right]\omega_c - \alpha_f\left[\omega_s tg(\Phi_r) - \frac{\theta_1(q) R I_o}{q} - j\omega_s\right] = 0 \tag{9}$$

2.2 – Dipole mode, on resonance

Assuming a resonator at $\omega_r = q\omega_0 + \omega_c$, we get:

$$\omega_c = \omega_s + j\frac{\alpha_f}{2}\left[1 - \sqrt{1 + 4\frac{\theta_1(q) R I_o}{q\alpha_f}}\right] \tag{10}$$

As expected, in the full coupling condition there is no real shift of the synchrotron frequency, whereas the imaginary shift gives the growth rate of the instability. We recognize in the term

$$\frac{q}{\theta_1(q) R I_o} = \tau_1 \tag{11}$$

the instability rise time usually obtained from eq. (3).

It is interesting to analyze two different regimes.

For $\tau_1 >> \tau_f$, we get:

$$\omega_c \approx \omega_s - j\frac{1}{\tau_1} \tag{12}$$

In this case the rise time given by eq.(11), can be considered a fairly good approximation.

Quite different results are obtained in the other case, namely when $\tau_1 << \tau_f$, for which we get:

$$\omega_c \approx \omega_s - \frac{j}{\sqrt{\tau_1 \tau_f}} \tag{13}$$

The effective rise time $\tau_{eff} = \sqrt{\tau_1 \tau_f}$ results to be the geometric mean of τ_1 and τ_f. One could conclude from the above equation that cavities characterized by an extremely long filling time, should be preferred as regards the multibunch instabilities. Expliciting the two terms in the rise time of eq.(13) we have:

$$\tau_{eff} = \left(\frac{2q}{\theta_1(q)\omega_r I_o (R/Q)} \right)^{\frac{1}{2}} \tag{14}$$

Therefore, in the regime $\tau_1 << \tau_f$ the effective rise time is inversely proportional to the square root of the ratio R/Q. By increasing Q and keeping R/Q constant, the effective rise time reaches an asymptotic value no more dependent on the cavity filling time.

As an example we plot in Fig. 1, as a function of Q, the growth rates $\alpha_1 = 1/\tau_1$ and $\alpha_{eff} = 1/\tau_{eff}$ computed for DAΦNE, assuming a parasitic resonance with R/Q=1Ω, at $\omega_r = 500\omega_0 + \omega_s$, exciting the motion of 30 bunches of 3 cm RMS length for a total current of 1.4 A. The upper curve is the growth rate $\alpha_1(Q)$ while the lower one is $\alpha_{eff}(Q)$. We note that at high Qs the difference between the two curves becomes larger and larger. In order to verify the correctness of eq.(10), we have reported on the same plots the instability growth rates (dots) obtained from the time domain simulation code[8] described in section 6. The numerical results agree quite well with those computed from eq.(10).

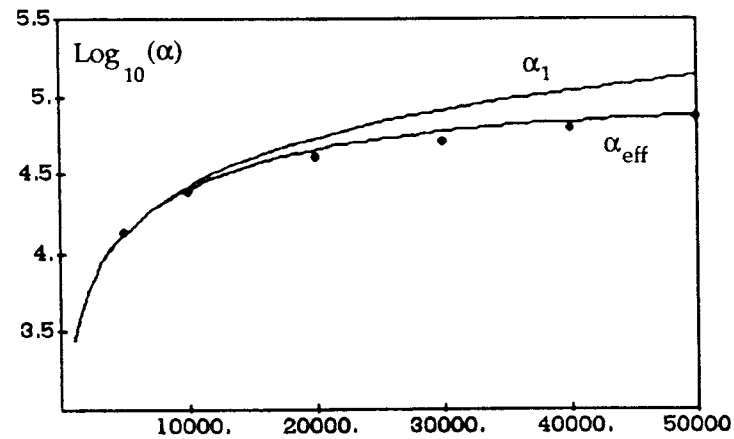

FIG. 1 – Growth rates α_1 (Q) and α_{eff} (Q), for an HOM with R/Q=1.

For the DAΦNE cavity only few undamped HOMs with a relatively high shunt impedance give a τ_{eff} significantly higher than τ_1. In Table II we report the results relative to the HOMs of the DAΦNE cavity given by URMEL[9]. The rise times computed with eq.(10)

are given for $\omega_p=\omega_r$ (full coupling). Analogous results for the measured HOMs of the cavity prototype are shown in Table IV. One can see that when the HOM is beated on resonance, the instability is extremely fast and uncurable, whereas for damped HOMs the rise time is much longer and, easely curable with a feedback system.

Table II – URMEL Cavity Modes

MONOPOLAR MODES				
MODE TYPE	FREQ. [MHz]	(R/Q) [Ω]	Q_0	τ_{eff} [μs]
0-EM-1	367.38	61.38	49100	
0-MM-1	695.97	15.81	49800	8
0-EM-2	794.85	0.01	81900	1850
0-MM-2	987.18	0.01	65900	2100
0-EM-3	1069.79	0.25	66900	96
0-EM-4	1119.92	2.11	57500	20
0-MM-3	1138.40	0.09	56800	270
0-EM-5	1203.83	0.79	67600	37
0-MM-4	1283.84	0.17	56200	150
0-EM-6	1318.43	0.77	72400	35
0-MM-5	1390.57	0.33	57800	81
0-EM-8	1481.07	0.85	55400	38
0-MM-7	1570.06	0.55	62200	51
0-EM-9	1574.96	0.88	61000	35
0-EM-10	1665.50	0.17	68200	136
0-MM-8	1672.18	1.12	63100	29
0-MM-9	1717.68	0.22	68500	109
0-EM-11	1742.33	0.21	57300	133
0-MM-10	1774.36	1.53	62400	24
0-EM-12	1796.49	0.13	56400	217
0-MM-11	1866.16	0.47	63300	62
0-EM-14	1955.71	0.15	91400	133
0-EM-15	2011.62	0.23	59500	132
0-MM-13	2038.39	0.24	64400	120

It must be said that Landau damping could have a noticeable effect on the instability, once the HOMs have been damped. In Fig. 2 we show the Q required for the 0-MM-1 cavity mode versus the bunch length. The damping time depends almost quadratically on the bunch length, and for bunches shorter than 3 cm a much stronger damping of the HOM would be required. Morover the real coherent shift could make it uneffective.

For sake of completeness, we point out that the growth rates have been worked out assuming an individual coupling of one sideband with a single resonator. These calculations neglect the superposition of the shunt impedance of several HOMs on the same relative mode. This effect can enhance (sum of shunt impedances) or reduce (difference of shunt impedance) the coupling. The time simulation code shows that for DAΦNE these effects are generally negligible, even in the presence of the HOM damping system.

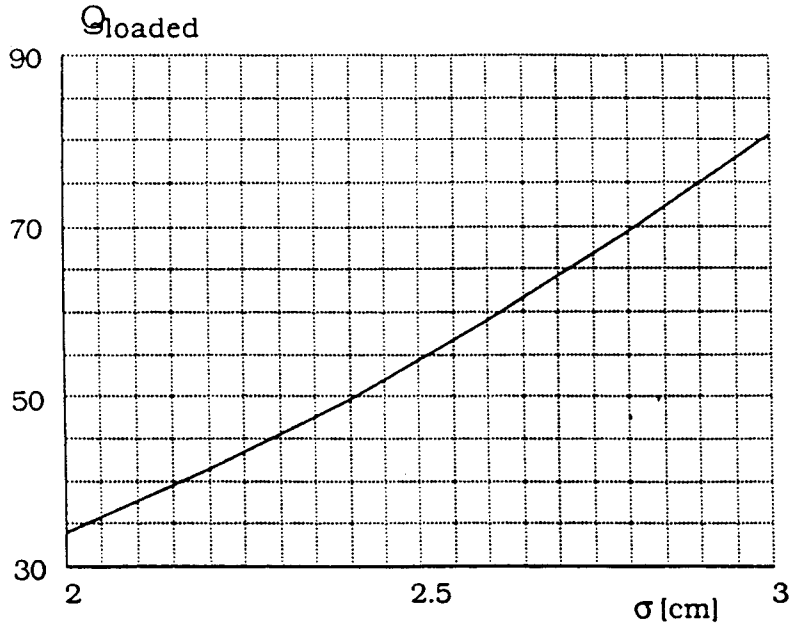

FIG. 2 – Q_L vs. bunch length for 0-MM-1 Landau Stability.

2.3 – Some considerations on high Qs cavity

The shortest rise time is given by the "on resonance" asymptotic value of τ_{eff}, that we call $\bar{\tau}_{eff}$, reached for $\tau_f >> \tau_1$, i.e. for HOMs characterized by very high Qs. It might happen that the machine parameters are such that $\bar{\tau}_{eff} > \tau_d$ (damping time).

Therefore, at a design stage, it is interesting to compare the effective rise time $\bar{\tau}_{eff}$ with the damping time τ_d due to radiation effect or to the Landau damping. If $\bar{\tau}_{eff} > \tau_d$, the beam is stable without any action on the RF cavity. As an example we give the condition to keep the beam stabilized by the radiation damping.

For short Gaussian bunches, it is useful to write down the effective rise time in the form:

$$\bar{\tau}_{eff} = \left(\frac{4(E/e)\omega_s}{I_o \alpha_c} \right)^{\frac{1}{2}} \frac{1}{\omega_r (R/Q)^{\frac{1}{2}}} \tag{15}$$

$\tau_1 << \tau_f$ requires that

$$Q\sqrt{R/Q} >> \sqrt{\frac{\omega_s (E/e)}{I_o \alpha_c}} \tag{16}$$

and $\bar{\tau}_{eff} > \tau_d$ gives

$$\omega_r \sqrt{R/Q} < \omega_o (U_o/e) \sqrt{\frac{\omega_s}{\pi^2 I_o \alpha_c (E/e)}} \tag{17}$$

The two relations above are never fulfilled in DAΦNE. However, for typical R/Q values, the conditions are better satisfied for superconducting cavities at very high energy, provided that the momentum compaction is very small.

2.4 – Dipole mode, off resonance

A problem arising in the standard calculation of ω_c is the following: as a consequence of the coupling to the imaginary part of the impedance, the sidebands ω_p shift toward the resonant angular frequency ω_r of the HOM; this shift leads to a stronger coupling with the resistive impedance and to a further shift of ω_p. Iterating this way of reasoning, every coupled sideband should always couple with the maximum shunt impedance. Fortunately, the right expression of ω_c in eq.(10) shows that the sideband finds a new equilibrium frequency.

A sample HOM with Q=10000, R/Q=1 and q=500, has been chosen to compare eq.(9) with the results of the time domain simulation code. Also in this case the agreement is quite satisfactory, as shown in Figs. 3a and 3b.

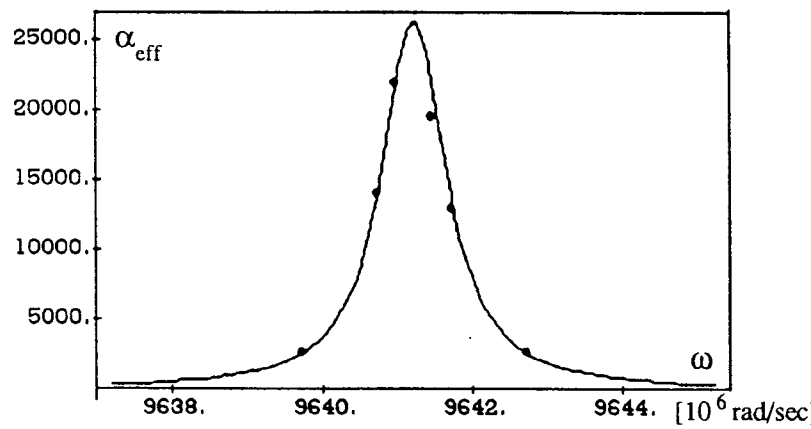

FIG. 3a – Growth rate $\alpha_{eff}(\omega)$ for R/Q=1, Q=10^4, q=500.

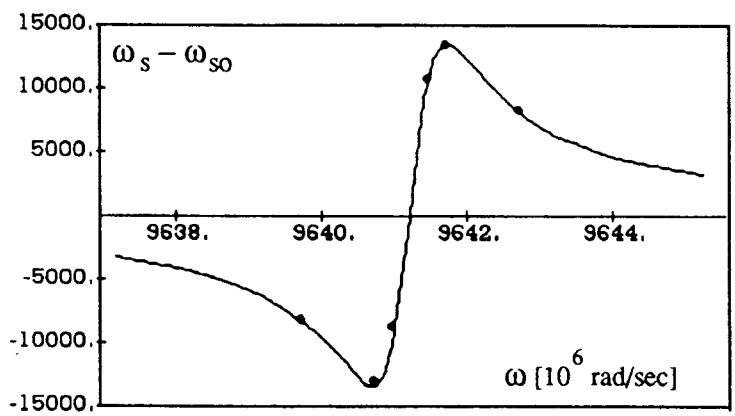

FIG. 3b – Angular frequency shift $\Delta\omega_s(\omega_r)$, for R/Q=1, Q=10^4, q=500.

3. – A CAVITY WITH LOW HOM CONTENTS

As a first remark, RF power requirements are not highly demanding in a storage rings like DAΦNE. At the operating energy of 510 MeV and beam current of 1.4 A in 30 bunches, a peak voltage up to 250 kV is required in the RF cavity, mainly to control the bunch length. The power dissipation in the cavity has to be kept reasonably low to ease the mechanical and cooling design. A shunt resistance as low as R=2MΩ ($V^2/2P$) for the fundamental mode seems indeed acceptable, what enables us to consider the minimization of the R/Q for the HOMs as the main goal of the design process. A strong reduction of R/Q values is pursued in view of several beam dynamics aspects:

— Power loss of the HOMs,
— Single bunch instability,
— Multibunch instabilities.

3.1 – Design procedure of cavity shape

The basic idea is to 'open' the beam tubes at the cavity irises in order to let the higher frequency parasitic modes propagate through them. This implies a strong reduction of the characteristic impedance of all the HOMs, except at most the lowest in frequency, which need a special care. A taper is then used as a gradual transition from the cavity iris to the ring vacuum pipe.

A careful analysis of the longitudinal wake potentials was made by means of the code TBCI[10], aiming to reduce the cavity contribution to the machine impedance[11]. As a result, a design with no beam tubes and two long tapers was proposed and the final comparison with a conventional design, with tubes and short tapers, showed a rather impressive difference in the loss factor to the HOMs (k_{pm} = 0.07 against 0.16 V/pC), while showing a slightly larger value of the R/Q at the fundamental mode. Since the total loss factor for a single bunch passage is

$$k_{pm} = \sum_{\text{all the HOMs}} \frac{\omega_r}{2}\left(\frac{R}{Q}\right)\exp\left(-\omega_r^2\sigma_t^2\right) \tag{18}$$

this means that on the average the R/Qs are decreased substantially. This fact was confirmed by a frequency-domain analysis (done by means of the codes OSCAR2D[12] and URMEL), where the presence of some strong HOMs above the beam tube cutoff was observed in the short tapered, but not in the long tapered structure.

The cavity design can noticeably influence the R/Q for the lower frequency modes . For example, it is impossible to maximize the R/Q for the accelerating mode 0-EM-1 and to minimize those for the two most dangerous HOMs (0-MM-1, 1-EM-1) simultaneously, as simple pill-box calculations have shown. This is true also when beam 'holes' are introduced, at least until the mode frequency remains below cutoff. Even if a noncylindrical but regular shape is used, a similar behaviour is reproduced in the simulations, although the definition of the accelerating gap becomes a bit arbitrary, since the evanescent field penetrates the beam tubes. Anyhow one can adjust the longitudinal dimension and the cavity shape to vary the strength of the 0-MM-1 mode and that of the 1-EM-1 alternatively.

Two quite popular examples of accelerating cavity are the so-called 'bell-shaped' (or 'rounded') cavity and the 'nosecone' cavity. In the latter the 'nosecones' are introduced to concentrate the electric field in the region of the beam, thus increasing the R/Q, but they help also to decrease the R/Q of the 0-MM-1 mode considerably, while the situation of the 1-EM-1 mode is worsened, because of the abrupt discontinuity. In the high-Q, 'rounded' structure, on the opposite, the smooth profile is beneficial for dipole modes, but retains a big value for the 0-MM-1 mode, which closely follows the behaviour of the accelerating mode. We have investigated both structures, trying to maintain the shunt resistance R = 2.5 ÷ 3 MΩ at the same operating frequency of 368 MHz. A comparison between the 2 structures is reported in Table III and shows a clear preference for the 'nosecone' cavity as regards the 0-MM-1 mode and for the 'rounded' cavity as regards the 1-EM-1 mode.

Table III – Nosecone vs. Rounded.

	Nosecone	Rounded		Nosecone	Rounded
Frequency (MHz)	368.3	368.3	0–MM–1 mode:		
R/Q (Ω)	69.9	61.7	Frequency (MHz)	704.7	696.8
Q	34000	49000	R/Q (Ω)	4.2	16.0
R_S (MΩ)	2.37	3.04	Q	30000	50000
k_l (V/pC)	0.101	0.129	R_S (kΩ)	128	800
k_0 (V/pC)	0.077	0.068	1–EM–1 mode:		
k_{pm} (V/pC)	0.024	0.061	Frequency (MHz)	565.0	532.7
k_t' (V/pC/m)	1.16	1.38	R'/Q (Ω)	30.3	13.7
k_{pm} / k_0	0.31	0.91	Q	42000	54000
k_t' / k_0 *1 mm	0.015	0.020	R'_S (MΩ)	1.28	0.74

For the other HOMs up to the cutoff the situation of the two cavities is quite similar, as displayed in Figs. 4a and 4b. We know from multibunch instability calculations that appropriate actions have to be taken anyway to strongly damp the 0-MM-1 mode, which is the most dangerous because it has the highest shunt impedance. Thus there is no more any clear reason to choose the 'nosecone' cell as our model cavity, while the 'rounded' cell is certainly to be preferred because it is of much easier construction and cooling. Also, it provides 3 MΩ of shunt resistance against the 2.5 MΩ of the 'nosecone' cavity, hence a bigger safety margin.

The final design is shown in Fig. 5. Much care has been taken to keep all HOM frequencies far away from harmonics of the bunch repetition rate in order to avoid resonant enhancement of the parasitic power loss.

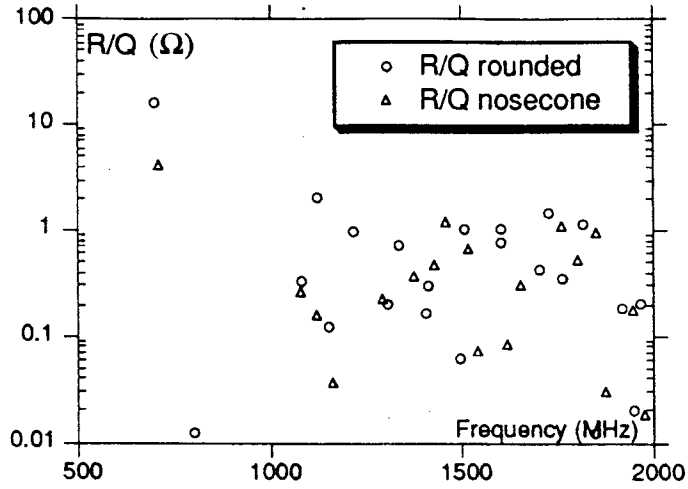

FIG. 4a – Characteristic impedances of the monopole modes.

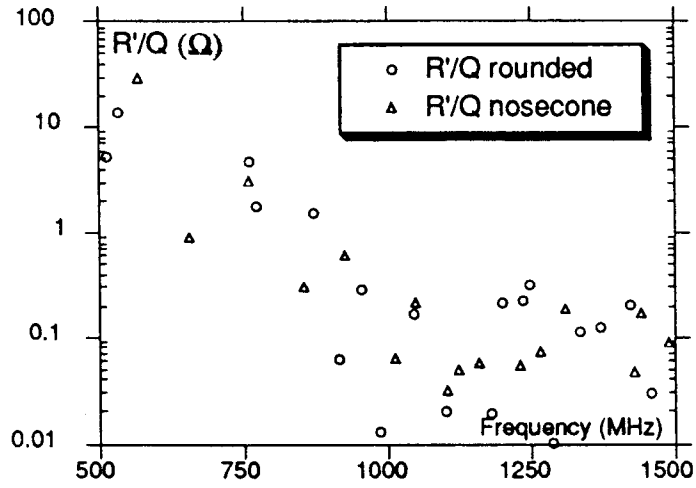

FIG. 4b – Characteristic impedances of the dipole modes.

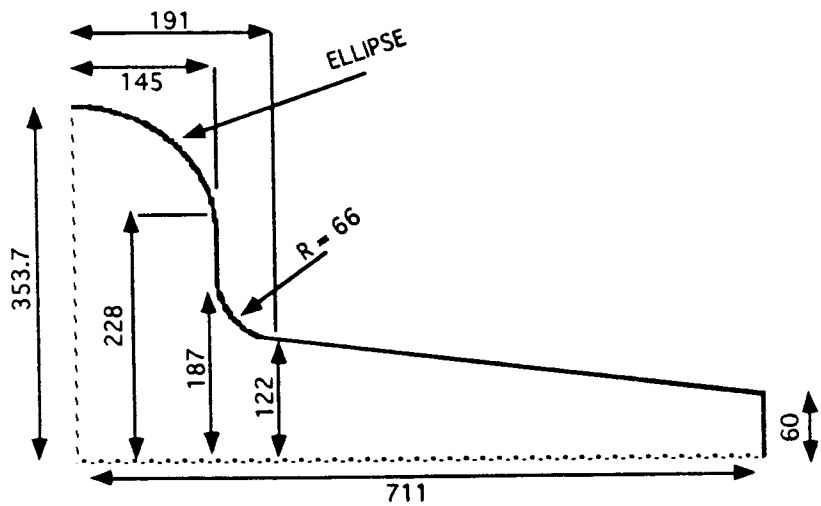

FIG. 5 – DAΦNE cavity shape and dimensions (mm).

4. – HOM DAMPING

The problem of parasitic mode damping in room temperature RF accelerating cavities for high current particle accelerators is being faced in other Laboratories[13,14] and the proposed or adopted solutions depend upon the accelerator demands.

A well known method to damp HOMs consists of coupling them out of the cavity by means of loops or antennas which are applied to the resonator surface in correspondence of the peaks of the parasitic fields and dissipating the extracted power on external 50 Ω loads through coaxial lines. As a rule, the transmission response of such devices must vanish at the cavity fundamental frequency not to extract the accelerating field energy; they require therefore some kind of tuning. The effectiveness of a loop/antenna coupler to damp a specific cavity mode can be excellent if its response has a maximum at the mode frequency.

HOM coupling can also be achieved by opening slots onto the cavity surface and conveying the fields out with waveguides (WG). Energy must then be dissipated by means of high losses materials applied in the vacuum environment or on external loads placed beyond a vacuum separation window. Being the WG a natural high-pass filter, the accelerating field remains trapped in the cavity providing that the WG cut-off is above the cavity fundamental mode (FM) frequency.

We have applied and tested both damping systems to some cavity models. The results obtained with the WGs have been more satisfactory due to the wide band WG response and their capability to reject the FM without any tuning device. We have then considered more practical to use WG dampers instead of loops or antennas.

4.1 – Waveguide to Cavity HOM coupling

Since the description of the e.m. fields in a resonant cavity loaded with impedance matched WGs has not satisfactorly been made by existing simulation codes so far, different approximate techniques have been developed to solve the problem. These methods[15, 16] allow to work out the most meaningful cavity parameters (as loaded Q values and beam longitudinal and transverse impedances) starting from the output data of 2 dimension (2D) and 3 dimension (3D) computer codes.

However, being the WG mode propagation carried out mainly in the TE_{10} mode, a general rule to optimize the damping effect is to open the WG slots onto the cavity surface in correspondence of the maximum intensity of the azimuthal HOM magnetic field Ho. The use of 2D and 3D codes is helpful to this investigation.

Once the location and the geometry of the cavity slots have been defined, the loaded Q values of the cavity HOMs can be roughly estimated if the unperturbed e.m. field existing before slotting the cavity wall, is considered the source of the guide propagating wave and the e.m field values normalized to the total energy content U are calculated with the code.

The current density source $\mathbf{J_s(r)}$ on the aperture surface S can be derived from the unperturbed magnetic field $\mathbf{H_o(r)}$ as:

$$\mathbf{J_s(r)} = \mathbf{n} \times \mathbf{H_0(r)} \text{ on the surface S} \tag{19}$$

where $\mathbf{n}$ is the outward unit vector normal to S.

Then, the WG magnetic field $\mathbf{H_w(r)}$ can be obtained from the magnetic Green Function of the waveguide $\mathbf{G_m(r,r')}$ accordingly to:

$$\mathbf{H}_w(\mathbf{r}) = \int_{s'} \mathbf{G}_m(\mathbf{r},\mathbf{r}')\mathbf{J}_s(\mathbf{r}')d^2\mathbf{r}' \tag{20}$$

The magnetic Green Function $\mathbf{G}_m(\mathbf{r},\mathbf{r}')$ for a rectangular WG is a 3 x 3 matrix whose analytical expression is known[17].

The magnetic field $\mathbf{H}_w(\mathbf{r})$ can be expanded in terms of normal modes propagating in the WG. Anyway, as long as the cavity mode has a frequency between 1st and 2nd WG mode cutoff, the sole non-evanescent term in the expansion (20) is the TE_{10} WG mode. Other expansion terms should be considered for mode frequencies above the 2nd WG mode cutoff. Even in this case, due to the symmetry of the source, the term associated to the WG TE_{10} mode is the most relevant one in the expansion; thus, we can conclude:

$$\mathbf{H}_w(\mathbf{r}) \approx \mathbf{H}_{TE10}(\mathbf{r}) \tag{21}$$

Assuming a perfectly matched WG, the total energy associated to the Poynting's vector is dissipated in the WG termination load, i.e.

$$P_w = \frac{1}{2}\int_{s'} \mathrm{Re}\left[\mathbf{E}_w \times \mathbf{H}_w^*\right] da = \frac{1}{2} Z_{TE10} \int_{s'} |H_{wt}|^2 \, da \tag{22}$$

where P_w is the power dissipated in the WG load, Z_{TE10} is the WG impedance, S' is the WG cross section and H_{wt} is the $\mathbf{H}_w$ transverse component.

Finally, the external Q of the cavity mode due to the loading of several WGs is given by:

$$Q_{ext} = \frac{\omega_r U}{\sum_i P_w} \tag{23}$$

The calculation of Q_{ext} becomes less accurate as the wavelength decreases with respect to the wider slot size. For a wavelength to slot size ratio close to unity, the computed and measured $Q_{ext} \approx Q_{loaded}$ values are in the same order of magnitude as shown in Table IV.

Table IV – Measured modes of the cavity prototype.

	UNLOADED MODES				LOADED MODES			
MODE	Freq.[MHz]	R/Q [Ω]	Q_0	τ_{eff} [μs]	Freq [MHz]	$Q_{L,Calc.}$	$Q_{L,Meas.}$	τ_{eff} [ms]
0-EM-1	357	61	25000		349.5		22000	
0-MM-1	747.5	16	24000	9	745.7	75	70	1.37
0-EM-2	796.8	0.5	40000	90	796.5	550	230	12.9
0-MM-2	1023.6	0.9	28000	60	1024.9	90	150	10.0
0-EM-3	1121.1	0.3	12000	370	1125.4	—	240	18.3
0-MM-3	1175.9	0.6	5000	440	1172.0	65	100	21.9
0-EM-4	1201.5	0.2	9000	730	1194.3	220	130	50.5
0-EM-5	1369.0	2.0	5000	135	1361.6	115	300	2.2
0-MM-4	1431.7	1.0	2000	670	1423.2	—	750	1.8
0-EM-6	1465.0	0.1	2000	6670	1467.6		190	71.2

4.2 – Cavity Damper Design

HOM damping can be optimized by placing the WGs in correspondence of a maximum of the surface field. This has been calculated with the code OSCAR2D as a function of the curvilinear coordinate *s* of the cavity profile (see Fig. 6) for some HOMs. The center of the cell profile is the curvilinear coordinate reference.

The highest R/Q mode 0-MM-1 has the magnetic field peak at s = 23 cm; some higher frequency modes have a maximum in the tapered tubes.

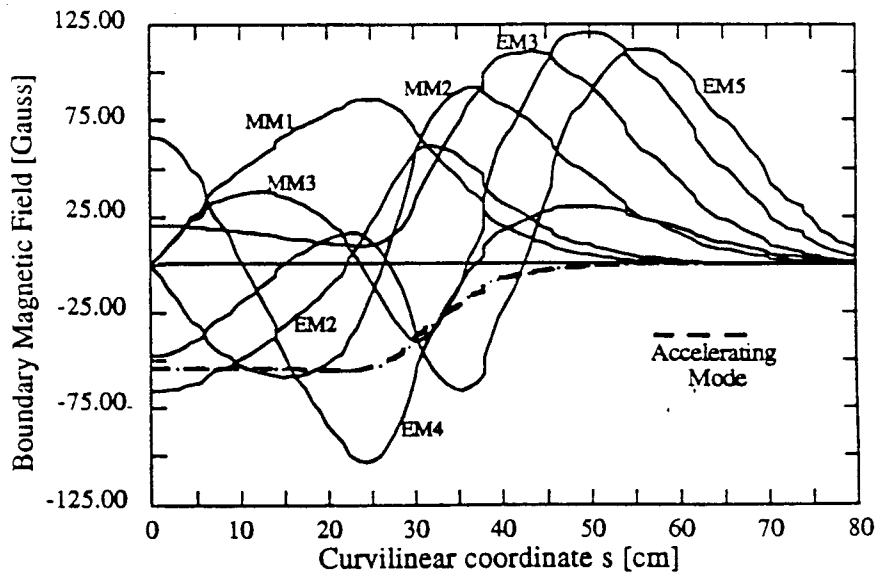

FIG. 6 – Surface Field Distribution of the Cavity Modes

To improve the damping of the 0-MM-1, without perturbing the FM symmetry, three WGs can be applied 120° apart at s = 23 cm onto the cavity surface. The WG cutoff frequency should be 500 MHz to allow the dipole modes 1-MM-1 and 1-EM-1, at 511 and 532 MHz respectively, to propagate.

Other modes can effectively be coupled by the WGs, as shown in fig. 6. One more WG with cut-off at 1070 MHz can be located onto each tapered tube where some high frequency HOMs penetrate and have magnetic field peak. The WGs on tapers can be rotated 90° apart to couple also the dipoles.

4.3 – Cavity Prototype Tests

A low power copper cavity model has been manufactured. Due to some mechanical imperfections of the model, the measured frequencies sligthly differ from those calculated with the codes but the HOM quality factors were high enough (in the order of some 10^4) to carry out reliable damping measurements.

An intense measurement program has been carried out to define the dimensions of the cavity main body WGs. Three WG shapes with equal cut-off have been considered. A set of 3 single ridge WGs of 200x40 mm^2 cross section and 70x25 mm^2 ridge has been connected to

the prototype and tested; both the FM frequency and the quality factor Q degradations were negligible due to the very small size of the ridge WGs.

Two sets of rectangular WGs of 305x40 and 305x50 mm^2 were also tested. In this case the larger WG size caused a degradation of both the FM frequency and Q but the HOM damping was better. The 305x40 mm^2 WG has been choosen being the best compromise between opposite requirements.

The WGs applied to the tapers have a 140x40 mm^2 rectangular cross section and do not degrade the FM since that field vanishes at those locations.

A picture of the cavity model is shown in Fig. 7.

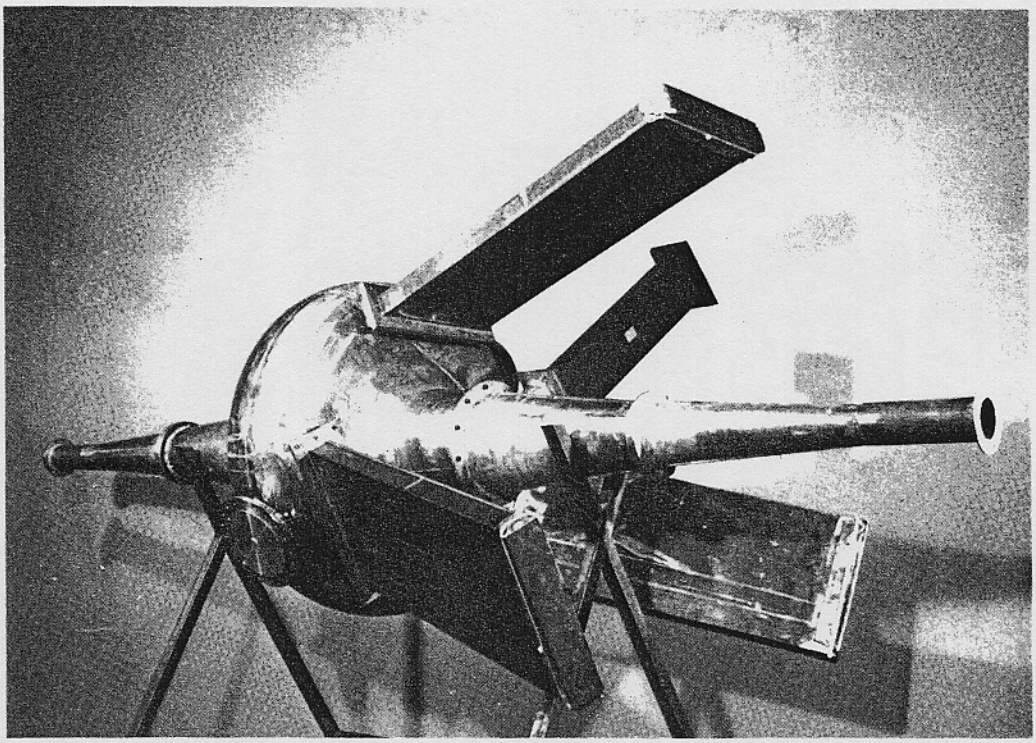

FIG. 7 – The DAΦNE Cavity Low Power Model.

A complete characterization up to 1.5 GHz of the cavity prototype fully equipped with WGs is reported in Table IV. Some HOM Qs have been estimated according to the method illustrated in section 4.1. The obtained HOM dampings are satisfactory and the expected rise times of the coupled bunch dipole mode instabilities seem compatible with the operation of a fast feedback system. The FM Q degradation, due to the evanescent field in the WGs is less than 15% and a frequency variation of about - 2% has been measured; therefore the outer diameter of the final cavity has been reduced by about 1 cm to have the unloaded FM frequency 2 % greater than the nominal value.

A mechanical sketch of the RF cavity proposed for DAΦNE is reported in Fig. 8. Three additional circular ports in the cavity main body allow to insert loops or antennas if more damping of particular modes will be needed.

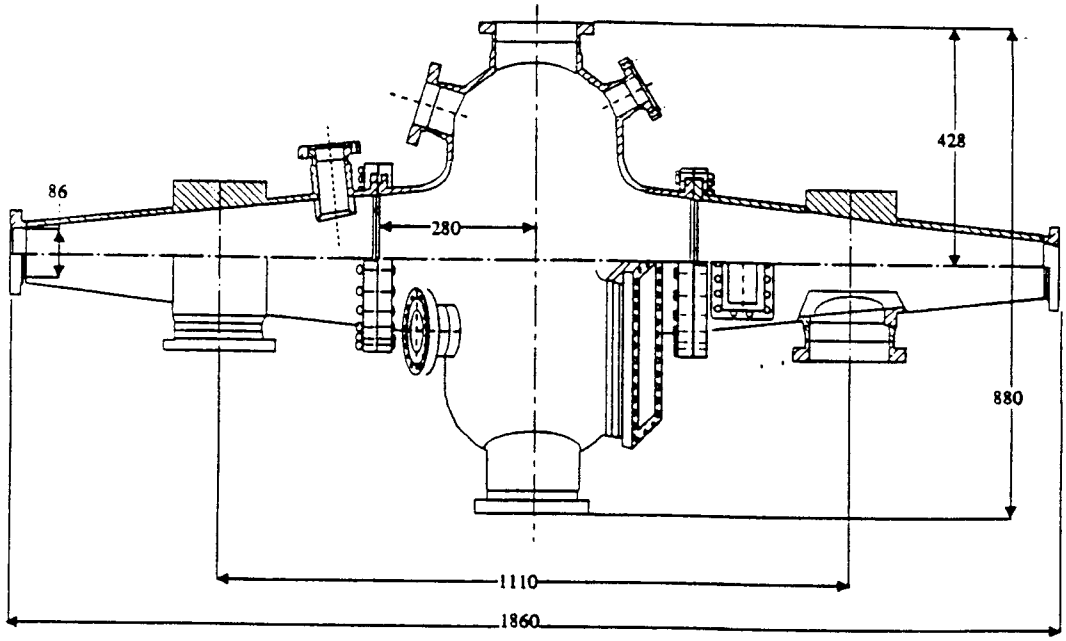

FIG. 8 – Sketch of the DAΦNE Cavity.

4.4 – Waveguide Termination Loads

The HOM power extracted from the cavity has to be dissipated on a dummy load placed at the WG far end. The most significant features of such a load should be low reflectivity on a broad frequency band and vacuum compatibility.

The beam power delivered to the cavity HOMs has been estimated for 30 bunch operation. This permits to evaluate the thermal load onto the absorbing materials.

The beam current can be expressed as a Fourier series:

$$i_b(t) = \sum_{m=-\infty}^{+\infty} I_m \exp[jm\omega_o t] \tag{24}$$

The total HOM power strongly depends on the cavity monopole spectrum and increases when the beam lines I_m overlap the cavity spectrum.

Such a power can be calculated as follows:

$$P_T = \sum_{m=o}^{+\infty} \sum_{\text{all the HOMs}} \frac{2(R/Q)QI_m^2}{1+Q^2\left(\frac{m\omega_o}{\omega_r} - \frac{\omega_r}{m\omega_o}\right)^2} \tag{25}$$

The probability that a beam spectrum line interacts with the resonator spectrum is very small for an undamped cavity, but the associated power loss can be very high. For a strongly damped cavity, as in our case, the probability of overlap is much higher but the resultant power loss is a moderate value.

To estimate the HOM power, the measured damped Qs of the cavity model have been considered. The HOM frequencies and R/Qs values were taken from the cavity code simulation. The maximum estimated total power results $P_T \approx 150$ W corresponding to an asymmetrical machine filling of 27 bunches (insted of 30), required to avoid ion trapping. A large power capability safety margin can then be assumed in designing the WG loads.

The termination loads must be highly loss materials placed either in the ultra high vacuum (UHV) or in air after an Al_2O_3 RF window.

Both RF and UHV characteristics of an absorbing material consisting of plain ferrite tiles have been obtained[18]. The results show that the UHV desorption of this material is compatible with the machine vacuum but the ferrite brazing to the UHV side requires some care.

The use of an Al_2O_3 RF window to make the air/vacuum interface can be an alternative solution but the frequency bandwitdh of such a window could not be wide enough to couple out all the HOM power up to the DAΦNE beam pipe cutoff frequency (≈ 2.5 GHz).

A novel and interesting solution to extract the cavity HOM power is a wide-band WG to coaxial transition which converts the WG TE_{10} mode to the TEM mode in a large frequency range (≈ 2.5 octaves) with very low power reflections (VSWR < 2). Such a device, under development at LNF, would allow to use commercial coaxial N type or 7/8" ceramic feedthroughs to transfer the RF power to an external 50 Ω load. In this case, the possibility of sampling the HOM beam power with a directional coupler connected to the transition coaxial output, is a very actractive by product.

5. – BUNCH BY BUNCH FEEDBACK

Analytical calculations show that a cavity with undamped HOMs may lead to coupled bunch instabilities with unmanageably fast rise time.

The effort made to damp the dangerous HOMs, has reduced the shunt impedance by a large amount; on the other hand, the probability for any given coupled mode frequency to overlap a detuned HOM is higher and for some modes the coupled bunch rise time is still faster than the natural damping.

In this section we describe the main features of the damping feedback system adopted for controlling the longitudinal instabilities in DAΦNE.

5.1 – The feedback layout

The system proposed is a bunch by bunch, time-domain feedback. This choice is common to other multibunch, high intensity machines[19]. In order to obtain the right phase of the correction signal, the detected synchrotron oscillation has to be processed by a proper filter. A frequency domain feedback needs a passband filter tuned onto every excited oscillation mode. For DAΦNE this would imply a large number of RF filters with a consequent complication of the whole system.

A bunch by bunch feedback allows to damp the individual motion of each bunch indipendently of the cause (e.g.: injection transient, beam-beam, HOMs) thus uncoupling its

motion from that of the other bunches. In principle, k_b parallel filters are needed to damp independently the motion of k_b bunches.

Available electronic technology allows the realization of a mixed analog/digital system employing Digital Signal Processors (DSP) as filters.

The main advantage of such system is that the same DSP can serve as a filter for several different bunches, thus reducing the overall complexity. Indeed, the use of programmable devices allows also the flexibility to program the gain and to tune the frequency response of the filter on-line according to the beam current intensity and to the machine parameters which affect the synchrotron motion.

The proposed scheme is the following: the synchrotron phase error of each individual bunch is detected by a longitudinal pick-up. The resulting signal is shifted by $\pi/2$ at the oscillation frequency by a proper digital filter, then the signal is amplified and an energy correction is applied via a longitudinal kicker.

In the smooth approximation the damping rate provided by the system is:

$$\alpha_{fb} = \frac{1}{4\pi}\omega_o \frac{\Delta U_{fb}}{\Delta E} \tag{26}$$

where ΔU_{fb} is the energy correction by the feedback kicker and ΔE is the instantaneous energy error.

The number of revolutions per synchrotron oscillation is very high, that means we have an overwhelming number of samples to reconstruct the phase error of the single bunch; in order to reduce the complexity of the feedback processing part (and the number of the DSP needed), the down sampling technique is adopted[20]. This consists in processing the detected signal after a certain number of turns.

5.2 – Front end

We need to measure the single bunch error with a phase detector; we do not use a narrow band tuned detector because any signal feed-through by the preceding bunches must be avoided.

The signal from a longitudinal pick up passes in a microstrip comb generator[21] in which a coherent burst of bipolar pulses can be produced. The phase of this pseudo sinusoidal signal with respect to the RF voltage is measured by means of a double balanced mixer in which the local oscillator is a harmonic of the ring radiofrequency.

The phase detector output goes into a fast digitizer (input bandwidth 1.2 GHz) capable of sampling the signal of individual bunches at full rate with 8-bit resolution.

5.3 – Digital filter

A demultiplexer distributes the digitized bunch signal to the proper DSP, which performs the filtering algorithm, producing the feedback correction. This correction signal is calculated by a Finite Impulse Response (FIR) filter with N taps where N is the number of samples with which we reconstruct the synchrotron oscillation.

The output signal is computed as the convolution sum of N preceding values of the input signals $\Delta\varphi_{n-i}$:

$$y(t_n) = G\sum_{i=1}^{N} \Delta\varphi(t_n - i)h_i \tag{27}$$

where h_i are the filter coefficients, and G is the feedback gain.

As shown in the simulations, the feedback system performs satisfactorily with a number of taps as small as 5. A preliminary estimate of the number DSP's needed for 30 bunches is ~ 5, assuming a DSP with an instruction time of 25 nsec. Different filter algorithms were also investigated and the best effectiveness is achieved with sinusoidal and highpass configurations.

The proposed architecture of the digital part exhibits good flexibility together with the minimum hardware complexity.

5.4 Longitudinal kicker.

The energy correction, in terms of the output power P_{fb} of the final amplifiers is

$$\Delta U_{fb} = \sqrt{2P_{fb}(RT^2)_k} \tag{28}$$

where $(RT^2)_k$ is the kicker shunt impedance, corrected by the transit time factor.

The bandwidth of the kicker must be at least $(k_b\omega_o/4\pi)$ in order to kick all bunches separately.

In order to reduce the power requirements of the final feedback amplifiers and the reflections due to mismatches at the power port, we are optimizing the design of the longitudinal kicker. The present choice is a series of two $\lambda/4$ strip lines with full coverage, connected with $\lambda/2$ delay lines. This arrangement must provide a peak shunt impedance of 400 Ω and a half power bandwidth in excess of 1/2 the bunch frequency.

From the simulation results, the power needed to damp the bunch oscillations at the maximum phase displacement, expected at the injection, is less than 500W.

6. – TIME DOMAIN SIMULATION CODE

The theoretical analysis presented in section 2 considers the coupling of a single sideband with a single parasitic resonance of the RF cavity. The bunches are assumed equally populated and equispaced.

A more general analysis could be done by considering many HOMs coupling to the full beam spectrum. Even including all the modes, it remains unpractical to study the beam dynamics under the conditions of unequally spaced and unequally populated bunches, as well as of large oscillations at injection and under the effect of the bunch-by-bunch feedback. These different scenarios are better investigated by means of a time domain simulation code properly developed[8].

The simulation code executes the tracks of the longitudinal motions of the bunches stored in DAΦNE, with the aim of including all the main phenomena affecting the beam dynamics (i.e. the bunch-by-bunch feedback,the effect of the HOMs, the synchrotron radiation).

Each bunch is modelled as a single particle of a given charge. With this condition it is possible to simulate dipole oscillations only.

Basically the core of the algorithm can be divided into three main parts:

1) propagation around the ring
2) feedback effect
3) beam-cavity interaction.

6.1 – Propagation around the ring

To describe the motion of a single bunch in the machine, we use the energy deviation ΔE and the phase $\Delta\varphi$.

In the propagation around the ring, each bunch loses energy due to the broad band impedance (U_{bb}) that does not depend on the energy of the bunch, and to synchrotron radiation (U_r) , for which we used the following linear expression

$$U_r = U_o\left(1+2\frac{\Delta E}{E}\right) \tag{29}$$

where U_o is the energy lost by a synchronous particle.

It is therefore possible to correlate the quantities ΔE and $\Delta\varphi$ just outside the RF cavity with those we find at the entrance of the feedback kicker at the following turn:

$$\begin{pmatrix}\Delta E\\ \Delta\varphi\end{pmatrix}_k = \begin{pmatrix}1-2\frac{U_o}{E} & 0\\ \frac{2\pi h\alpha_c}{E} & 1\end{pmatrix}\begin{pmatrix}\Delta E\\ \Delta\varphi\end{pmatrix}_{rf} - \begin{pmatrix}U_o+U_{bb}\\ 0\end{pmatrix} \tag{30}$$

where α_c is the momentum compaction, h is the harmonic number, 'k' means at the entrance of the kicker and 'rf ' outside the RF cavity.

6.2 – The feedback effect

HOM damping is not sufficient to get the beam stable by itself. A powerful longitudinal feedback is necessary to damp oscillation modes and the injection transient.

In the program the feedback described in section 5 is simulated in all its parts. It is possible to change the system configuration and the feedback gain by means of the input file. Different digital filters as delay line, high and low pass, derivative and sinusoidal filters have been also investigated.

6.3 – Beam-cavity interaction

The cavity is simulated as a series of parallel RLC circuits that represent the HOMs. When a charge q_b crosses the cavity, it perturbs the voltage of each mode. Since the beam loading in the fundamental cavity mode is very heavy, RF cavity feedback will be necessary to compensate it. In simulations to date, we have assumed the compensation is perfect, i.e. the fundamental mode voltage is given by

$$V_g = \hat{V}_g\cos(\Delta\varphi) \tag{31}$$

with $\hat{V}_g$ the peak generator voltage.

The induced voltage for each mode is a kick ΔV depending on the shunt resistance R and the quality factor Q of that mode. In order to take into account the bunch length (we suppose that the bunch has a gaussian distribution), the shunt resistance is corrected by a factor equal to

$$\exp\left[-(\omega_r \sigma_t)^2\right] \tag{32}$$

where σ_t is the RMS bunch duration.

With the purpose of following the behavior of the induced wake voltage of each mode in a matrix form, we use the conjugated variables v(t) and the current in the inductance i(t). Between the passage of two bunches, the voltage of each mode executes free oscillations represented by the homogeneous solution of the differential equation of an RLC parallel circuit. Therefore we have[22]

$$\begin{pmatrix} v(t) \\ i(t) \end{pmatrix} = \exp\left(-\alpha_f t\right) \begin{pmatrix} \cos(\beta t) - \frac{\alpha_f}{\beta}\sin(\beta t) & -\frac{\omega_r R}{\beta Q}\sin(\beta t) \\ \frac{\omega_r Q}{\beta R}\sin(\beta t) & \cos(\beta t) + \frac{\alpha_f}{\beta}\sin(\beta t) \end{pmatrix} \begin{pmatrix} v(t_o) \\ i(t_o) \end{pmatrix} \tag{33}$$

where β is the natural angular frequency and $v(t_o)$ and $i(t_o)$ are the starting conditions.

When a bunch crosses the cavity, we increase v(t) by the kick ΔV and continue the propagation. The total energy gained by the bunch in the RF cavity is therefore

$$E_c = e\left(V_g + \sum_{\text{all the HOMs}} \left[v(t) + \frac{1}{2}\Delta V\right]\right) \tag{34}$$

where the last term takes into account the fundamental theorem of beam loading: a bunch sees half of the wake voltage it induces during its passage.

6.4 Application to DAΦNE.

We have performed different simulations with all the HOMs measured values of the waveguide loaded cavity as given in Table IV.

Since the frequency may vary during the machine operation, we have chosen to simulate the worst case, i.e. all the HOMs are in full coupling with the unstable sidebands of the beam spectrum.

First, we have observed the instabilities with the feedback off, by simulating the injection of the 30th bunch (with an error of 100 psec) assuming all the others in the equilibrium state. Fig. 9 shows the oscillations of a perturbed bunch and Fig. 10 shows the oscillations of the injected bunch during the first 5000 turns.

Then we have found a feedback configuration such as to damp the oscillations with a kicker voltage of 400 Volt, as we can see in Figs. 11 and 12.

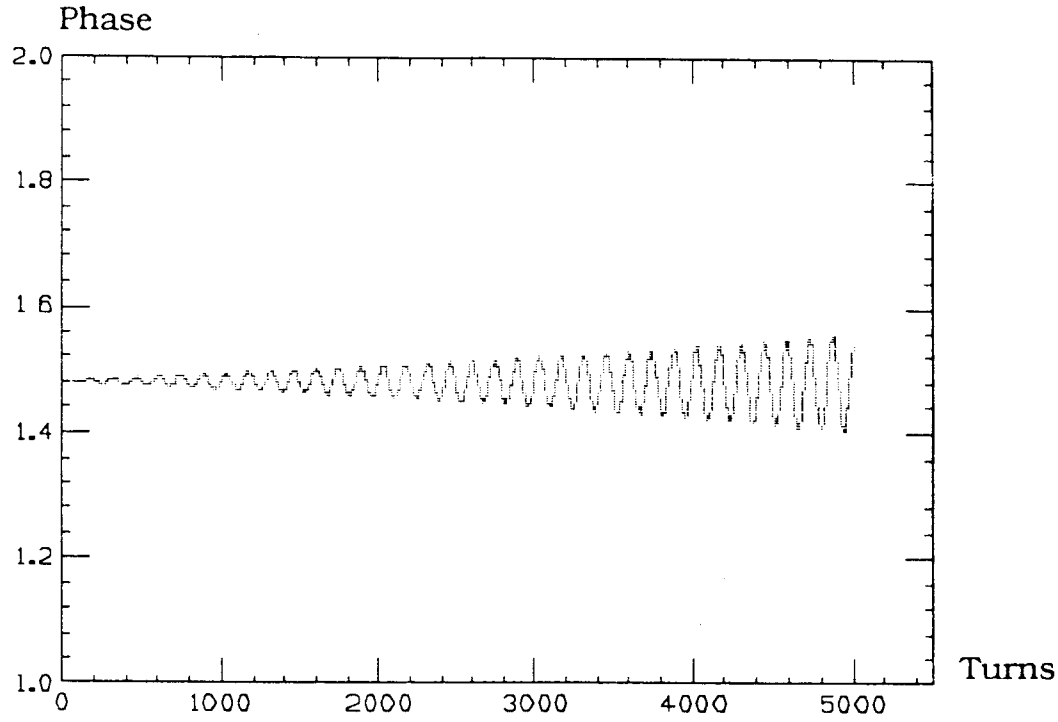

FIG. 9 – Oscillations of a perturbed bunch.

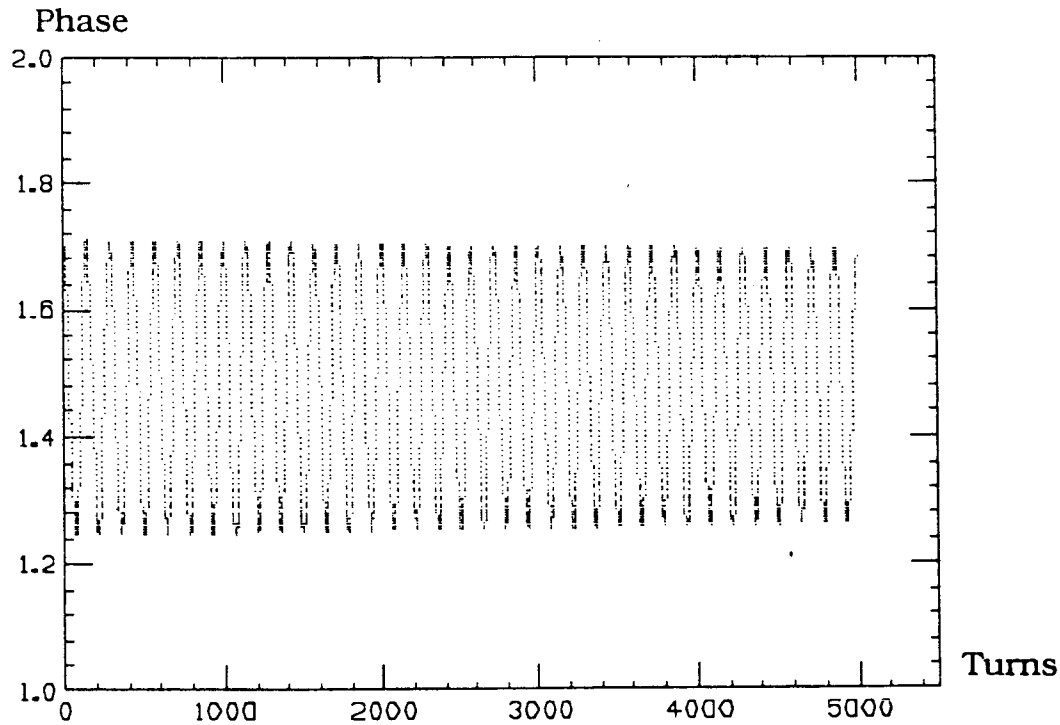

FIG. 10 – Oscillations of the injected bunch.

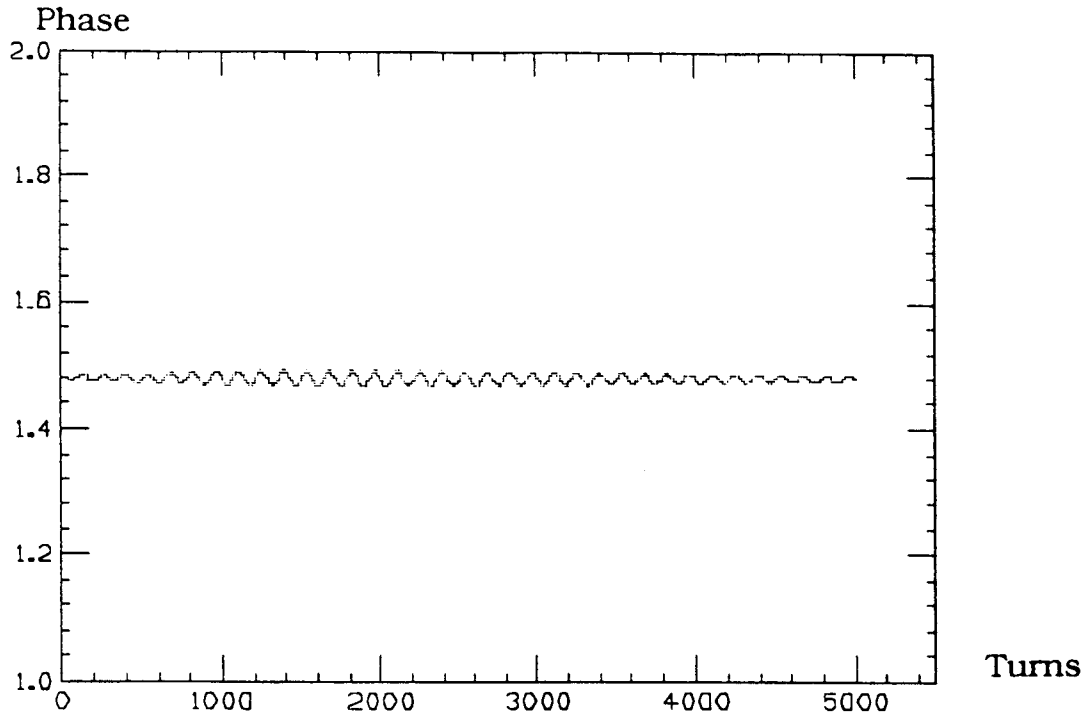

FIG. 11 – Oscillations of a perturbed bunch with the feedback on.

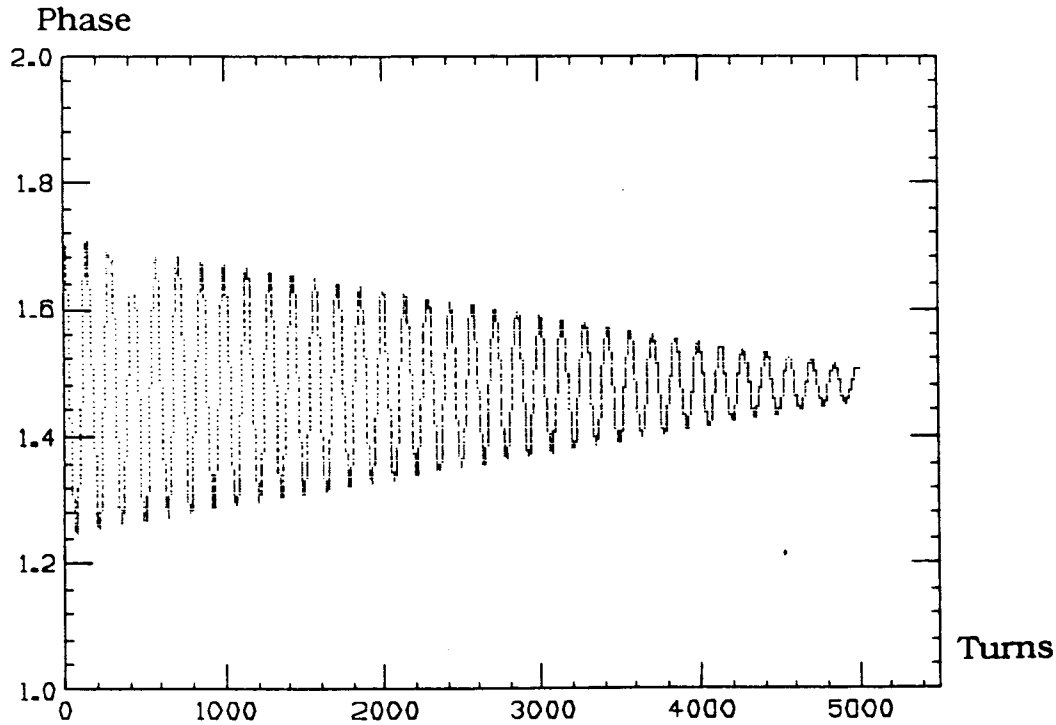

FIG. 12 – Oscillations of the injected bunch with the feedback on.

To be sure that the injection of the 30th bunch was the most dangerous for the stability point of view, with the same feedback parameters, we have simulated the injection of the nth bunch with n-1 bunches at the equilibrium phase. In Fig. 13 we show the maximum phase excursion of the bunch more perturbed by this injection versus the number of the bunch injected. As expected the oscillations becomes larger increasing the total current already stored.

Comparison of results obtained by a similar code developed at SLAC[23,24] showed some inconsistencies in the case of low Q of the HOMs. We presume that this is due to the approximations on the wake field expressions, valid only for high Qs, adopted in the SLAC code.

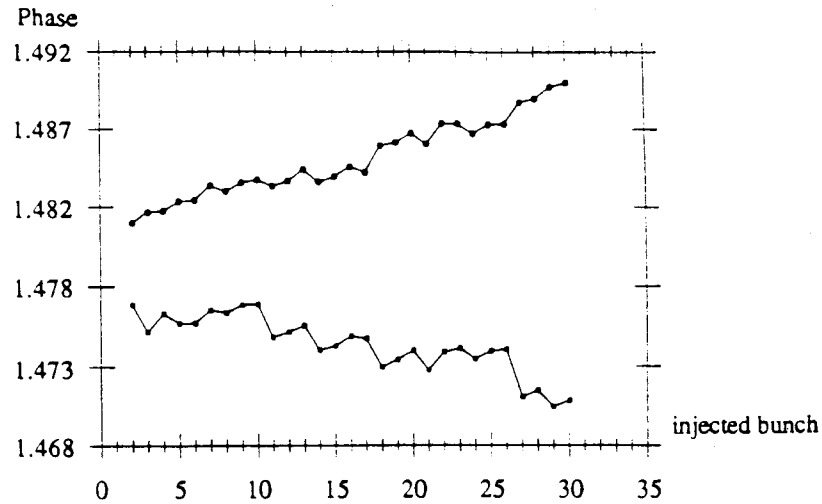

FIG. 13 – Maximum perturbation of the stored bunches.

7. – CONCLUSIONS

Multibunch instabilities are certainly one of the main problem to solve to reach a very high luminosity in DAΦNE. We made a strong effort on the analysis of the methods that could take these instabilities under control. We are reasonably confident that by properly damping the resonant fields in the machine, we will be able to damp the residual instability by means of a feedback system.

8. – ACKNOWLEDGMENTS

We are pleased to acknoledge the collaboration and the hospitality provided to some of us by all the members of PEP-II group, in particular John Fox and Gerard Oxoby. We also like to thank Bruno Zotter and Albert Hofmann for the very useful discussions and suggestions on the subject of this paper.

REFERENCES

1. G. Vignola, *DAΦNE: the Frascati Φ-Factory*, Proc. of the 1991 Part. Acc. Conference, Vol. 1, pp. 68-70, S. Francisco, may 1991.
2. F. Sacherer, *IEEE Trans. NS* **24** (1977) 1393, also CERN/PS-BR/77 5 and 6.
3. J. L. Laclare, CERN 87-03, Vol. I, pp. 264-326.
4. M.S. Zisman et al., LBL 21270.
5. A. Hoffman at al.. *IEEE Trans. NS* **26** (1979) 3514.
6. A. Hoffmann and B Zotter, private communication.
7. M. Migliorati and L. Palumbo, *Multibunch Instabilities in DAΦNE. Longitudinal and Transverse Coherent Frequency Shift*, DAΦNE Technical Note G-18, (1993).
8. M.Bassetti, et al., *A Time Domain Simulation Code of the Longitudinal Multibunch Instabilities*, DAΦNE Technical Note, G-19, (1993).
9. T. Weiland, *NIM* **216** (1983), pp. 329-348.
10. T. Weiland, *NIM* **212** (1983), pp. 13-34.
11. S. Bartalucci, et al., *A low loss cavity for the DAΦNE Main Ring*, DAΦNE Technical Note G-6, (1991).
12. P. Fernandes and R. Parodi, *IEEE Trans. on Magn.* **21**(6) (1985) 2246.
13. R.Rimmer et al., *An RF Cavity for the B-Factory*, SLAC-PUB-6129, April 1993.
14. A.Massarotti, et al., *Particle Accelerator* **35**, pp. 167-175 (1991).
15. N.Kroll and D.Yu, *Particle Accelerators* **34**, pp. 231-250 (1990).
16. P.Arcioni and G.Conciauro, *Particle Accelerators* **36**, pp. 177-203 (1991).
17. R.Collin, *Field Theory of Guided Waves*, McGraw-Hill Book Company, Inc. , New York Toronto London (1960).
18. R.Boni, et al., *Study of Parasitic Mode Absorbers for the Frascati F-Factory RF Cavities* LNF-93/014 (P), April 1993.
19. *An Asymmetric B-Factory*, LBL PUB-5303.
20. H. Hindi et al, *Down Sampled Signal Processing for a B Factory Bunch-by-Bunch Feedback System*, Proceedings of EPAC 92.
21. J. D. Fox, et al., *Feedback Implementation Options and Issues for B Factory Accelerators*, SLAC-PUB-5932, Sept 1992.
22. M. Bassetti, *Finite Difference Equations Calculations of Beam-Cavity Coupling Instability*, LNF Note 67/45, Frascati (1967).
23. D. Briggs, et al., *Computer Modelling of Bunch-by-Bunch Feedback for the SLAC B-Factory Design*, IEEE Particle Accelerator Conference, San Francisco (1991).
24. K. A. Thompson, *Simulation of Longitudinal Coupled-Bunch Instabilities*, ABC-24, (1991).